# Free Vibration Analysis of Simply Supported Orthotropic Square Plates with a Square Hole

異方性有孔板の自由振動問題の一解析法

M. Huang [*1], T.Sakiyama [*2], H. Matsuda [*3], C. Morita [*4], S.Q. Ma [*5]
黄 美, 崎山 毅, 松田 浩, 森田 千尋, 馬秀琴

[*1]Member of JSCE, Dr.of Eng., Res. Assoc., Dept.of Struct. Eng. Nagasaki Univ. (852-8521, Nagasaki)
[*2]Member of JSCE, Dr.of Eng., Prof., Dept.of Struct. Eng. Nagasaki Univ. (852-8521, Nagasaki)
[*3]Member of JSCE, Dr.of Eng., Assoc.Prof., Dept.of Struct. Eng. Nagasaki Univ. (852-8521, Nagasaki)
[*4]Member of JSCE, Dr.of Eng., Assoc.Prof., Dept.of Struct. Eng. Nagasaki Univ. (852-8521, Nagasaki)
[*5]Lecturer, Dept.of Mech. Eng. Yanshan Univ., P.R.China

An approximate method is extended for analyzing the free vibration problem of simply supported orthotropic square plate with a square hole. In this paper, a square plate with a square hole is transformed into an equivalent square plate with non-uniform thickness by considering the hole as an extremely thin part of the equivalent plate. Therefore, the dynamic characteristics of a plate with a hole can be obtained by analyzing the equivalent plate. The Green function, which is the discrete solution for the deflection of the equivalent plate, is used to obtain the characteristic equation of the free vibration. The effects of the side to thickness ratio, hole side to plate side ratio and the variation of the thickness on the frequencies are considered. Some numerical analyses are carried out for the simply supported orthotropic square plate with a square hole. The efficiency and accuracy of the numerical solutions by the present method are investigated.

***Key Words :*** *approximate method, square plate with a square hole, equivalent square plate, Green function, vibration*

## 1. Introduction

Plates with holes are extensively used in aeronautical, mechanical and civil structures to lighten the structure and to obtain the convenient connection of structural members. Their dynamic characteristics have been studied for many years. Most previous investigations have been confined to isotropic plates with holes [1–5]. The study of composite plates with holes are rather limited. Reddy [6] studied the large amplitude free vibration of layered composite plates with rectangular cutouts by finite element method. Frequencies corresponding to linear and nonlinear situations were presented for thin and thick orthotropic and laminated composite plates. Avalos, Larrondo and Laura [7] obtained the frequency parameters for anisotropic rectangular plates with free-edge holes by using the Rayleigh-Ritz method. The effects of aspect ratio, hole side to plate side ratio and the position of the hole on the frequencies were investigated. However, in these studies the effect of the variation of the thickness on frequencies was not considered.

This paper extends the early work [8] to analyze the free vibration of orthotropic square plates with a hole. By considering the hole as an extremely thin part of a plate, the free vibration problem of a plate with a hole can be transformed into the free vibration problem of its equivalent square plates with non-uniform thickness. Green function, which is the discrete solution for the deflection of the equivalent plate, is used to obtain the characteristic equation of the free vibration. The effects of side to thickness ratio, hole side to plate side ratio and the variation of the thickness in one direction or two directions on the frequencies are presented. The lowest 5 frequency parameters and their mode shapes are given for simply supported orthotropic square plates with a square hole. By comparing the present results with those previously reported, the convergence and accuracy of the present method are investigated.

## 2. Discrete Green Function

An $xyz$ coordinate system is used in the present study with its $x-y$ plane contained in middle plane of an orthotropic square plate and the $z-$axis perpendicular to the middle plane of the plate. The thickness and the length of the orthotropic square plate are $h$ and $a$, respectively. The principle material axes of the plate in the direction of longitudinal, transverse and normal directions are designated as 1, 2 and 3. The differential equations of the plate with a concentrated load $\overline{P}$ at point $(x_q, y_r)$ are as follows:

$$
\begin{aligned}
&\frac{\partial Q_x}{\partial x}+\frac{\partial Q_y}{\partial y}=-\overline{P}\delta(x-x_q)\delta(y-y_r),\\
&\frac{\partial M_x}{\partial x}+\frac{\partial M_{xy}}{\partial y}-Q_x=0,\\
&\frac{\partial M_y}{\partial y}+\frac{\partial M_{xy}}{\partial x}-Q_y=0,\\
&M_x=D_{11}\frac{\partial \theta_x}{\partial x}+D_{12}\frac{\partial \theta_y}{\partial y}+D_{16}(\frac{\partial \theta_x}{\partial y}+\frac{\partial \theta_y}{\partial x}),\\
&M_y=D_{12}\frac{\partial \theta_x}{\partial x}+D_{22}\frac{\partial \theta_y}{\partial y}+D_{26}(\frac{\partial \theta_x}{\partial y}+\frac{\partial \theta_y}{\partial x}),\\
&M_{xy}=D_{16}\frac{\partial \theta_x}{\partial x}+D_{26}\frac{\partial \theta_y}{\partial y}+D_{66}(\frac{\partial \theta_x}{\partial y}+\frac{\partial \theta_y}{\partial x}),\\
&Q_y=kA_{44}(\frac{\partial w}{\partial y}+\theta_y)+kA_{45}(\frac{\partial w}{\partial x}+\theta_x),\\
&Q_x=kA_{45}(\frac{\partial w}{\partial y}+\theta_y)+kA_{55}(\frac{\partial w}{\partial x}+\theta_x),
\end{aligned}
\tag{1}
$$

where $Q_x$ and $Q_y$ are the transverse shear forces, $M_x$ and $M_y$ are the bending moments, $M_{xy}$ is the twisting moment, $k=5/6$ is the shear correction factor, $\delta(x-x_q)$ and $\delta(y-y_r)$ are Dirac's delta functions, $A_{ij}$ are the extensional stiffnesses $(i,j=4,5)$, $D_{ij}$ are the bending stiffnesses $(i,j=1,2,6)$.

$A_{ij}, D_{ij}$ can be obtained by the following expressions:

$$
\begin{aligned}
&A_{ij}=Q_{ij}h,\quad D_{ij}=\frac{1}{12}Q_{ij}h^3,\\
&Q_{11}=\frac{E_1}{1-\nu_{12}\nu_{21}},\quad Q_{22}=\frac{E_2}{1-\nu_{12}\nu_{21}},\\
&Q_{12}=\frac{\nu_{12}E_2}{1-\nu_{12}\nu_{21}},\quad Q_{44}=G_{23},\quad Q_{55}=G_{31},\\
&Q_{66}=G_{12},\quad \text{others } Q_{ij}=0,
\end{aligned}
$$

where $E_1$ is the axial modulus in the 1-direction, $E_2$ is the axial modulus in the 2-direction, $\nu_{12}$ is the Poisson's ratio associated with loading in the 1-direction and strain in the 2-direction, $\nu_{21}$ is the Poisson's ratio associated with loading in the 2-direction and strain in the 1-direction, $G_{23}, G_{31}$ and $G_{12}$ are the shear moduli in 2-3, 3-1 and 1-2 planes.

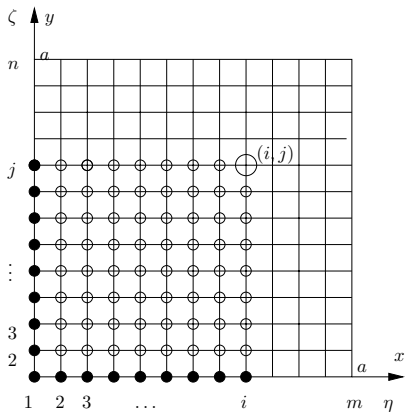


**Fig. 1** Discrete points on a rectangular plate

By using the non-dimensional expressions

$$
\begin{aligned}
&[X_1, X_2]=\frac{a^2}{D_0(1-\nu_{12}\nu_{21})}\,[Q_y, Q_x]\,,\\
&[X_3, X_4, X_5]=\frac{a}{D_0(1-\nu_{12}\nu_{21})}\,[M_{xy}, M_y, M_x]\,,\\
&[X_6, X_7, X_8]=\left[\theta_y, \theta_x, \frac{w}{a}\right],\quad [\eta,\zeta,\xi]=\left[\frac{x}{a},\frac{y}{a},\frac{z}{h}\right],
\end{aligned}
$$

the equation (1) can be rewritten as

$$
\begin{aligned}
\sum_{s=1}^{8}\{&F_{1ts}\frac{\partial X_s}{\partial \zeta}+F_{2ts}\frac{\partial X_s}{\partial \eta}+F_{3ts}X_s\}\\
&+P\delta(\eta-\eta_q)\delta(\zeta-\zeta_r)\delta_{1t}=0,
\end{aligned}
\tag{2}
$$

where $t=1\sim 8$, $P=\overline{P}a/(D_0(1-\nu_{12}\nu_{21}))$, $D_0=Eh_0^3/(12(1-\nu_{12}\nu_{21}))$ is the standard bending rigidity, $h_0$ is the standard thickness of the plate, $\delta_{ij}$ is Kronecker's delta, $F_{1ts}$, $F_{2ts}$ and $F_{3ts}$ are given in Appendix A.

By dividing a rectangular plate vertically into $m$ equal-length parts and horizontally into $n$ equal-length parts as shown in Figure 1, the plate can be considered as a group of discrete points which are the intersections of the ($m$+1)-vertical and ($n$+1)-horizontal dividing lines. In this paper, the rectangular area, $0\le\eta\le\eta_i$, $0\le\zeta\le\zeta_j$, corresponding to the arbitrary intersection $(i,j)$ as shown in Figure 1 is denoted as the area $[i,j]$, the intersection $(i,j)$ denoted by ◯ is called the main point of the area $[i,j]$, the intersections denoted by ∘ are called the inner dependent points of the area, and the intersections denoted by • are called the boundary dependent points of the area.

By integrating the equation (2) over the area $[i,j]$, the following integral equation is obtained:

$$
\sum_{s=1}^{8}\left\{F_{1ts}\int_0^{\eta_i}[X_s(\eta,\zeta_j)-X_s(\eta,0)]d\eta\right.
$$

$$+F_{2ts}\int_0^{\zeta_j}[X_s(\eta_i,\zeta)-X_s(0,\zeta)]d\zeta$$
$$+F_{3ts}\int_0^{\eta_i}\int_0^{\zeta_j}X_s(\eta,\zeta)d\eta d\zeta\Big\}$$
$$+Pu(\eta-\eta_q)u(\zeta-\zeta_r)\delta_{1t}=0, \quad (3)$$

where $u(\eta-\eta_q)$ and $u(\zeta-\zeta_r)$ are the unit step functions.

Next, by applying the numerical integration method, the simultaneous equation for the unknown quantities $X_{sij}=X_s(\eta_i,\zeta_j)$ at the main point $(i,j)$ of the area $[i,j]$ is obtained as follows:

$$\sum_{s=1}^{8}\Big\{F_{1ts}\sum_{k=0}^{i}\beta_{ik}(X_{skj}-X_{sk0})$$
$$+F_{2ts}\sum_{l=0}^{j}\beta_{jl}(X_{sil}-X_{s0l})$$
$$+F_{3ts}\sum_{k=0}^{i}\sum_{l=0}^{j}\beta_{ik}\beta_{jl}X_{skl}\Big\}$$
$$+Pu_{iq}u_{jr}\delta_{1t}=0, \quad (4)$$

where $\beta_{ik}=\alpha_{ik}/m, \beta_{jl}=\alpha_{jl}/n$, $\alpha_{ik}=1-(\delta_{0k}+\delta_{ik})/2$, $\alpha_{jl}=1-(\delta_{0l}+\delta_{jl})/2$, $t=1\sim 8$, $i=1\sim m$, $j=1\sim n$, $u_{iq}=u(\eta_i-\eta_q)$, $u_{jr}=u(\zeta_j-\zeta_r)$.

The solution $X_{pij}$ of the simultaneous equation (4) is obtained as follows:

$$X_{pij}=\sum_{t=1}^{8}\Big\{\sum_{k=0}^{i}\beta_{ik}A_{pt}[X_{tk0}-X_{tkj}(1-\delta_{ik})]$$
$$+\sum_{l=0}^{j}\beta_{jl}B_{pt}[X_{t0l}-X_{til}(1-\delta_{jl})]$$
$$+\sum_{k=0}^{i}\sum_{l=0}^{j}\beta_{ik}\beta_{jl}C_{ptkl}X_{tkl}(1-\delta_{ik}\delta_{jl})\Big\}$$
$$-A_{p1}Pu_{iq}u_{jr}, \quad (5)$$

where $p=1\sim 8$, $A_{pt}$, $B_{pt}$ and $C_{ptkl}$ are given in Appendix B.

In the equation (5), the quantity $X_{pij}$ at the main point $(i,j)$ of the area $[i,j]$ is related to the quantities $X_{tk0}$ and $X_{t0l}$ at the boundary dependent points of the area and the quantities $X_{tkj}$, $X_{til}$ and $X_{tkl}$ at the inner dependent points of the area. With the spreading of the area $[i,j]$ according to the regular order as $[1,1]$, $[1,2]$, $\cdots$, $[1,n]$, $[2,1]$, $[2,2]$, $\cdots$, $[2,n]$, $\cdots$, $[m,1]$, $[m,2]$, $\cdots$, $[m,n]$, a main point of a smaller area becomes one of the inner dependent points of the following larger areas. Whenever the quantity $X_{pij}$ at the main point $(i,j)$ is obtained by using the equation (5) in the above mentioned order, the quantities $X_{tkj}$, $X_{til}$ and $X_{tkl}$ at the inner dependent points of the following larger areas can be eliminated by substituting the obtained results into the corresponding terms of the right side of equation (5).

By repeating this process, the equation $X_{pij}$ at the main point is only related to the quantities $X_{rk0}$ ($r$=1,3,4,6,7,8) and $X_{s0l}$ ($s$=2,3,5,6,7,8) which are six independent quantities at the each boundary dependent point along the horizontal axis and the vertical axis in Figure 1, respectively. The result is as

$$X_{pij}=\sum_{d=1}^{6}\Big\{\sum_{f=0}^{i}a_{pijfd}X_{rf0}+\sum_{g=0}^{j}b_{pijgd}X_{s0g}\Big\}$$
$$+\overline{q}_{pij}P, \quad (6)$$

where $a_{pijfd}$, $b_{pijgd}$ and $\overline{q}_{pij}$ are given in Appendix C.

The equation (6) gives the discrete solution of the fundamental differential equation (2) of the bending problem of a plate under a concentrated load, and the discrete Green function is chosen as $X_{8ij}/[\overline{P}a/D_0(1-\nu_{12}\nu_{21})]$.

## 3. Integral Constant and Boundary Condition of a Square Plate

The integral constants $X_{rfo}$ and $X_{sog}$ involved in the discrete solution (6) are all quantities at the discrete points along the edges $\zeta=0$ ($y=0$) and $\eta=0$ ($x=0$) of the square plate. There are six integral constants at each discrete point. Half of them are self-evident according to the boundary conditions along the edges $\zeta=0$ and $\eta=0$ and half of them are needed to determine by the boundary conditions along the edges $\zeta=1$ and $\eta=1$.

The integral constants and the boundary conditions for a simply supported square plate are shown in Figure 2, and those at the corners of plate are shown in the boxes.

## 4. Equivalent Square Plate of a Square Plate with a Square Hole

A square plate with a hole can be transformed into an equivalent square plate with non-uniform thickness (shown in Figure 3) by considering the hole as an extremely thin part of the plate theoretically. The thickness of the actual part of original square plate is expressed as $h$, and the thickness of the extremely thin part of the equivalent square plate is expressed as $h_t$. The thickness of the plate along the border line between the actual part and the extremely thin part is chosen as $(h+h_t)/2$. In this paper, numerical results are carried out for a simply supported square plate

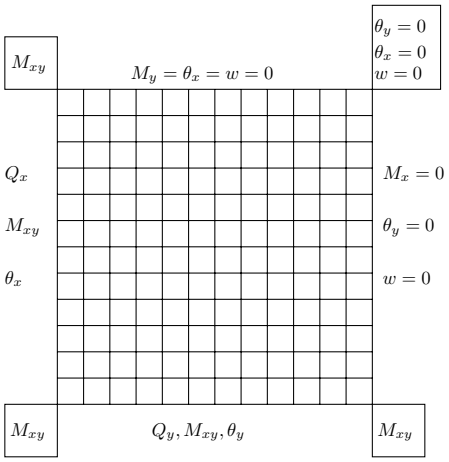


**Fig. 2** Simply supported plate

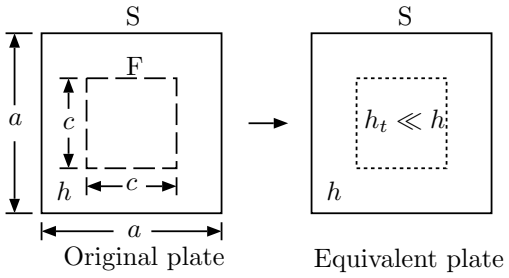


**Fig. 3** Square plate with a square hole and its equivalent square plate

with a central square hole. The simply supported and free edges are denoted by the symbols S and F, respectively, and shown by solid line and dotted line.

## 5. Characteristic Equation of Free Vibration of Square Plate with Non-uniform Thickness

By applying the Green function $w(x_0, y_0, x, y)/\overline{P}$ which is the displacement at a point $(x_0, y_0)$ of a plate with a concentrated load $\overline{P}$ at a point $(x, y)$ and point support at each discrete point $(x_c, y_d)$, the displacement amplitude $\hat{w}(x_0, y_0)$ at a point $(x_0, y_0)$ of the square plate during the free vibration is given as follows:

$$\hat{w}(x_0, y_0) = \int_0^a \int_0^a \rho h \omega^2 \hat{w}(x, y)[w(x_0, y_0, x, y)/\overline{P}]dxdy, \tag{7}$$

where $\rho$ is the mass density of the plate material.

The non-dimensional expressions are used as

$$\lambda^4 = \frac{\rho_0 h_0 \omega^2 a^4}{D_0(1-\nu_{12}\nu_{21})}, H(\eta, \zeta) = \frac{\rho(x, y)}{\rho_0}\frac{h(x, y)}{h_0},$$

$$G(\eta_0, \zeta_0, \eta, \zeta) = \frac{w(x_0, y_0, x, y)}{a}\frac{D_0(1-\nu_{12}\nu_{21})}{\overline{P}a},$$

$$W(\eta, \zeta) = \frac{\hat{w}(x, y)}{a},$$

where $\rho_0$ is the standard mass density.

By using the numerical integration method, equation (7) is discretely expressed as

$$kW_{kl} = \sum_{i=0}^{m}\sum_{j=0}^{n} \beta_{mi}\beta_{nj}H_{ij}G_{klij}W_{ij}, k = 1/(\mu\lambda^4). \tag{8}$$

From equation (8) homogeneous linear equations in $(m+1)\times(n+1)$ unknowns $W_{00}$,$W_{01}$,$\cdots$,$W_{0n}$, $W_{10}$,$W_{11}$ $\cdots$,$W_{1n}$,$\cdots$ $W_{m0}$,$W_{m1}$,$\cdots$,$W_{mn}$ are obtained as follows:

$$\sum_{i=0}^{m}\sum_{j=0}^{n} (\beta_{mi}\beta_{nj}H_{ij}G_{klij} - k\delta_{ik}\delta_{jl})W_{ij} = 0,$$
$$(k = 0, 1, \cdots, m, l = 0, 1, \cdots, n). \tag{9}$$

The characteristic equation of the free vibration of a square plate with variable thickness is obtained from the equation (9) as follows:

$$\begin{vmatrix} \mathbf{K_{00}} & \mathbf{K_{01}} & \mathbf{K_{02}} & \cdots & \mathbf{K_{0m}} \\ \mathbf{K_{10}} & \mathbf{K_{11}} & \mathbf{K_{12}} & \cdots & \mathbf{K_{1m}} \\ \mathbf{K_{20}} & \mathbf{K_{21}} & \mathbf{K_{22}} & \cdots & \mathbf{K_{2m}} \\ \vdots & \vdots & \vdots & \ddots & \vdots \\ \mathbf{K_{m0}} & \mathbf{K_{m1}} & \mathbf{K_{m2}} & \cdots & \mathbf{K_{mm}} \end{vmatrix} = \mathbf{0}, \tag{10}$$

where

$$\mathbf{K_{ij}} = \beta_{mj}\begin{bmatrix} \beta_{n0}H_{j0}G_{i0j0} - k\delta_{ij} & \cdots & \beta_{nn}H_{jn}G_{i0jn} \\ \beta_{n0}H_{j0}G_{i1j0} & \cdots & \beta_{nn}H_{jn}G_{i1jn} \\ \beta_{n0}H_{j0}G_{i2j0} & \cdots & \beta_{nn}H_{jn}G_{i2jn} \\ \vdots & \vdots & \vdots \\ \beta_{n0}H_{j0}G_{inj0} & \cdots & \beta_{nn}H_{jn}G_{injn} - k\delta_{ij} \end{bmatrix}.$$

## 6. Numerical Results

The convergence and accuracy of numerical solutions are investigated for simply supported isotropic and orthotropic plates with holes for the cases of uniform thickness and variable thickness in one or two directions. The orthotropic plate is made from graphite/epoxy. The material properties of isotropic and orthotropic plates are shown in Table 1. The convergent results of frequency parameter can be obtained by using Richardson's extrapolation formula for two cases of divisional numbers $m$ (=$n$).

### 6.1 Convergence of the Solution

In order to examine the convergence, numerical calculation is carried out by varying the number of divi-

**Table 1** Material properties of isotropic and orthotropic plates

| Material | $\frac{E_1}{E_2}$ | $\frac{G_{12}}{E_2}$ | $\frac{G_{13}}{E_2}$ | $\frac{G_{23}}{E_2}$ | $\nu$ |
|---|---|---|---|---|---|
| isotropic | 1 | 0.385 | 0.385 | 0.385 | 0.3 |
| orthotropic | 40 | 0.5 | 0.5 | 0.5 | 0.25 |

sions $m$ and $n$. The lowest 5 natural frequency parameters of an isotropic square plate with a square hole are shown in Table 2. It can be noticed that convergent results of frequency parameter can be obtained by using Richardson's extrapolation formula for two cases of divisional numbers $m$ (=$n$) of 12 and 16. Table 3 is used to determine the suitable thickness ratio $h/h_t$ of the original and extremely thin parts. It is sufficient to set the thickness ratio $h/h_t = 12$.

By the same method, the number of divisions $m(= n)$ and the thickness ratio $h/h_t$ can be determined for the other plates.

### 6.2 Accuracy of the Solution

The frequencies of the free vibration of square plates with square holes are given to show the accuracy of the numerical solution obtained by the present method. The lowest 5 natural frequencies and mode shapes of these plates are presented for the cases of uniform thickness and variable thickness.

**(1) Plate with Uniform Thickness**

Numerical values for the lowest 5 natural frequency parameter $\lambda$ of SSSS isotropic thin square plates with a square hole are given in Table 4 with the FEM values obtained by Ali and Atwal [4] and Kaushal and Bhat [9]. These results agree closely. From Table 4, the effects of the hole size on the first 5 frequencies for the SSSS isotropic thin square plate can be found. It might be noted that the variations of the fundamental and higher frequencies with hole size are quite different. As the ratio $c/a$ increases, the fundamental frequency first decreases a little , then increases. For $c/a = 0.5$, the fundamental frequency of the plate is higher than the corresponding frequency for the plate without a hole. But as the ratio $c/a$ increases, the second, third and fourth frequencies first increase a little, then decrease. For $c/a = 0.5$, these frequencies are lower than the corresponding frequencies for the plate without a hole. The fifth frequency monotonously decreases with the increase of $c/a$.

Table 5 presents the numerical results for the lowest 5 natural frequency parameter $\lambda$ of the SSSS orthotropic thin and moderately thick square plates

**Table 2** The natural frequency parameter $\lambda$ of SSSS isotropic square plate with a square hole and uniform thickness for various divisional number $m(= n)$ $(h/h_t = 12)$

| | | Mode sequence number | | | | |
|---|---|---|---|---|---|---|
| $m$ | Source | 1st | 2nd | 3rd | 4th | 5th |
| 8 | Present | 4.673 | 6.782 | 6.782 | 9.675 | 10.342 |
| 12 | Present | 4.726 | 6.585 | 6.585 | 8.619 | 9.483 |
| 16 | Present | 4.768 | 6.528 | 6.528 | 8.544 | 9.204 |

**Table 3** The natural frequency parameter $\lambda$ of SSSS isotropic square plate with a square hole and uniform thickness for various thickness ratio $h/h_t$ $(m = n = 16)$

| | | Mode sequence number | | | | |
|---|---|---|---|---|---|---|
| $h/h_t$ | Source | 1st | 2nd | 3rd | 4th | 5th |
| 2 | Present | 4.965 | 7.105 | 7.105 | 8.912 | 10.028 |
| 6 | Present | 4.776 | 6.564 | 6.564 | 8.815 | 9.270 |
| 12 | Present | 4.768 | 6.528 | 6.528 | 8.544 | 9.204 |
| 14 | Present | 4.767 | 6.526 | 6.526 | 8.415 | 9.199 |

**Table 4** The first five frequencies versus the ratio $c/a$ for SSSS isotropic square plate with a square hole and uniform thickness $(a/h = 100, h/h_t = 12)$

| | | Mode sequence number | | | | |
|---|---|---|---|---|---|---|
| $c/a$ | Source | 1st | 2nd | 3rd | 4th | 5th |
| 0 | Present | 4.548 | 7.188 | 7.188 | 9.011 | 10.146 |
| | Ref. [4] | 4.558 | 7.246 | 7.264 | 9.365 | 10.163 |
| | Ref. [9] | 4.529 | 7.110 | 7.110 | 9.001 | 10.034 |
| 0.1 | Present | 4.544 | 7.193 | 7.193 | 9.002 | 10.143 |
| | Ref. [4] | 4.403 | 7.174 | 7.194 | 9.235 | 9.891 |
| 0.2 | Present | 4.485 | 7.276 | 7.276 | 9.109 | 10.135 |
| | Ref. [4] | 4.397 | 7.017 | 7.017 | 8.968 | 9.662 |
| | Ref. [9] | 4.482 | 7.022 | 7.022 | 8.867 | 9.882 |
| 0.3 | Present | 4.507 | 6.785 | 6.785 | 9.133 | 9.776 |
| | Ref. [4] | 4.478 | 6.797 | 6.797 | 8.739 | 9.768 |
| 0.4 | Present | 4.588 | 6.612 | 6.612 | 8.899 | 9.483 |
| | Ref. [4] | 4.653 | 6.569 | 6.569 | 8.611 | 9.386 |
| 0.5 | Present | 4.822 | 6.455 | 6.455 | 8.448 | 8.845 |
| | Ref. [4] | 4.936 | 6.502 | 6.502 | 8.525 | 8.881 |
| | Ref. [9] | 4.979 | 6.542 | 6.542 | 8.667 | 8.875 |

with a square hole of side ratio $c/a = 0.5$. By comparing with the results of Reddy [6], the accuracy of the present results is investigated. Table 5 shows the side-to-thickness ratio $a/h$ affects the frequency considerately. The nodal patterns of the 5 modes of the

**Table 5** Natural frequency parameter $\lambda$ for SSSS orthotropic square plate with a square hole and uniform thickness ($c/a = 0.5, h/h_t = 12$)

| | | Mode sequence number | | | | |
|---|---|---|---|---|---|---|
| $a/h$ | Source | 1st | 2nd | 3rd | 4th | 5th |
| 100 | Present | 7.098 | 8.539 | 9.070 | 10.528 | 13.979 |
| | Ref. [6] | 7.160 | – | – | 10.598 | – |
| 10 | Present | 6.473 | 7.634 | 7.841 | 9.240 | 11.273 |
| | Ref. [6] | 6.537 | – | – | 9.139 | – |

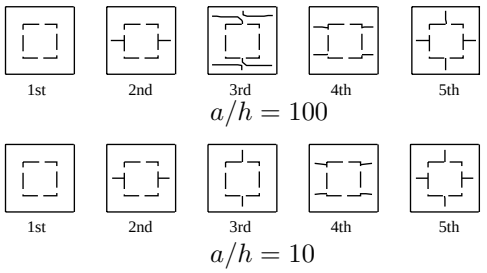


**Fig. 4** Nodal patterns for SSSS orthotropic square plate with a square hole and uniform thickness($c/a = 0.5, h/h_t = 12$).

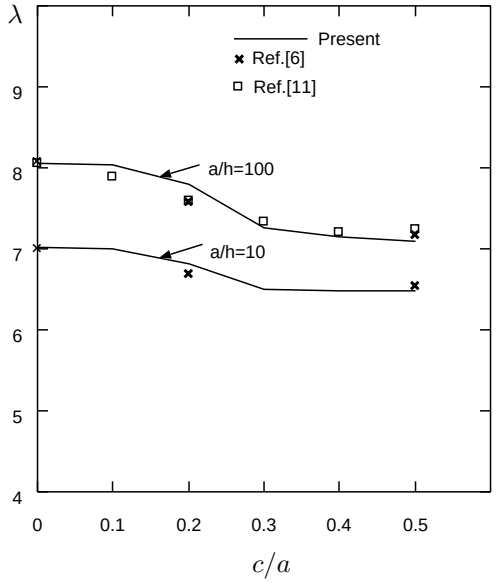


**Fig. 5** The fundamental frequency versus the ratio $c/a$ for SSSS orthotropic square plate with a square hole and uniform thickness.

plates are shown in Figure 4. It can be noted when $a/h$ changes from 100 to 10, the 1st, 2nd, 4th and 5th mode shapes don't change but the 3rd mode shape changes a lot.

To better illustrate the effect of the hole size on the frequency of SSSS orthotropic thin and moderately thick plate, the variation of fundamental frequency with $c/a$ is shown in Figure 5. It can be seen that the frequencies decrease with the increase of $c/a$ for both the thin and moderately thick plates. The effect of the transverse shear deformation on frequencies decreases with the increase of $c/a$. The present results agree closely with the results obtained by Lam, Hung and Chow [10] and Reddy [6] shown in Figure 5. Comparing the results of the fundamental frequencies of isotropic and orthotropic plates with $c/a = 0.5$ shown in Table 4 and Figure 5, respectively, it can be noted that the fundamental frequency decreases a little first and then increases with $c/a$ for isotropic plate, while it decreases with $c/a$ for orthotropic plate. To explain the phenomenon, two effects introduced by a hole are considered. The first one is a reduction in the strain energy of the plate which will decrease the frequency of the plate. The second one is a reduction in the mass which will increase the frequency. For the isotropic plate with a small hole, the first effect might be the dominant effect, and the frequency would decrease. But for a larger hole, the second effect might become the primary effect, and the frequency would begin to increase. Further explain can be found in [4]. In this paper, no apparent decrease of the first frequency can be shown for isotropic plate. The first frequency decreases just a little first and then increases in Table 4. For the orthotropic plate with a larger hole, the first effect might be still the dominant effect due to its high ratio of $E_1/E_2$, and the frequency would continue to decrease with $c/a \leq 0.5$.

Figure 6 shows the variation of the fundamental frequency parameter with the side-to-thickness ratio $a/h$ for the plates with $c/a$=0, 0.2 and 0.5. Isotropic and orthotropic cases are considered. The results of Reddy [6] are included in this Figure. It can be noticed that the effect of transverse shear deformation is much more pronounced in orthotropic plate than in isotropic plate. Also, the effect increases with the decrease of the ratio $a/h$. So as the ratio $a/h$ increases, the fundamental frequencies show non-linear increase for values of $a/h$ smaller than 30 but show linear increase for larger values of $a/h$ and keep constant for large values of $a/h$. The fundamental frequency parameter for the plate with side ratio $c/a = 0.2$ is lower than that of plate without a hole for both the isotropic and orthotropic cases. Compared with the frequencies of the plates with $c/a = 0$ and $c/a = 0.2$,

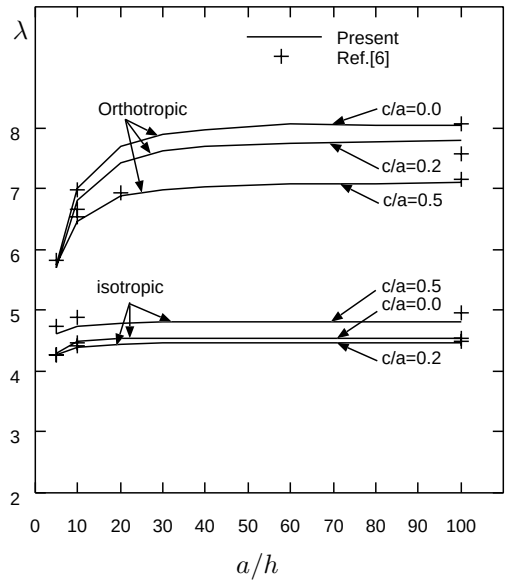


**Fig. 6** The fundamental frequency versus the thickness ratio $a/h$ for SSSS square plate with a square hole and uniform thickness ($h/h_t = 12$).

the frequency of the plate with $c/a = 0.5$ is higher for the isotropic case but it is lower for the orthotropic case.

### (2) Plate with Variable Thickness in One Direction

In order to investigate the accuracy of the present method for the plate with variable thickness, numerical values for the lowest 5 natural frequency parameter $\lambda$ of SSSS isotropic thin square plate with variable thickness in one direction are given in Table 6 with the results of Appl and Byers [11]. In this paper, variable thickness in one direction varies linearly along the $y$-direction according to the equation $h(x, y) = h_0(1 + \alpha y/a)$. From Table 6, it can be seen the method described can be also used to solve the vibration problem of the plate with variable thickness.

As application of the present method, the numerical results for the lowest 5 natural frequency parameter $\lambda$ of SSSS orthotropic thin and moderately thick square plates with a square hole of side ratio $c/a = 0.5$ and variable thickness in one direction are presented in Tables 7 and 8. From these Tables, it can be noticed that the frequency parameters will increase with the increase of $\alpha$. The nodal patterns of the 5 modes of the plates are shown in Figures 7 and 8. With the increase of $\alpha$, the horizontal nodal lines move down in both Figures.

**Table 6** Natural frequency parameter $\lambda$ for SSSS isotropic square plate with variable thickness in one direction ($a/h_0 = 100, h_0/h_t = 12$)

| | | Mode sequence number | | | | |
|---|---|---|---|---|---|---|
| $\alpha$ | Source | 1st | 2nd | 3rd | 4th | 5th |
| 0.1 | Present | 4.660 | 7.363 | 7.363 | 9.312 | 10.390 |
| | Ref. [11] | 4.661 | – | – | – | – |
| 0.8 | Present | 5.354 | 8.406 | 8.439 | 10.685 | 11.747 |
| | Ref. [11] | 5.335 | – | – | – | – |

**Table 7** Natural frequency parameter $\lambda$ for SSSS orthotropic square plate with a square hole and variable thickness in one direction ($c/a = 0.5, a/h_0 = 100, h_0/h_t = 12$)

| | | Mode sequence number | | | | |
|---|---|---|---|---|---|---|
| $\alpha$ | Source | 1st | 2nd | 3rd | 4th | 5th |
| 0.0 | Present | 7.098 | 8.539 | 9.070 | 10.528 | 13.979 |
| | Ref. [6] | 7.160 | – | – | 10.598 | – |
| 0.1 | Present | 7.267 | 8.749 | 9.299 | 10.782 | 14.045 |
| 0.8 | Present | 8.217 | 10.110 | 10.571 | 12.388 | 15.710 |

**Table 8** Natural frequency parameter $\lambda$ for SSSS orthotropic square plate with a square hole and variable thickness in one direction ($c/a = 0.5, a/h_0 = 10, h_0/h_t = 14$)

| | | Mode sequence number | | | | |
|---|---|---|---|---|---|---|
| $\alpha$ | Source | 1st | 2nd | 3rd | 4th | 5th |
| 0.0 | Present | 6.473 | 7.634 | 7.841 | 9.240 | 11.273 |
| | Ref. [6] | 6.537 | – | – | 9.139 | – |
| 0.1 | Present | 6.584 | 7.755 | 7.917 | 9.368 | 10.431 |
| 0.8 | Present | 7.206 | 8.456 | 8.565 | 10.151 | 10.784 |

### (3) Plate with Variable Thickness in Two Directions

The numerical results for the lowest 5 natural frequency parameter $\lambda$ of the SSSS orthotropic thin and moderately thick square plates with a square hole of side ratio $c/a = 0.5$ and variable thickness in two directions are presented in Tables 9 and 10. The thickness of the plate varies in the $x, y$-directions according to the sinusoidal function given by $h(x, y) = h_0(1 - \alpha \sin \pi x/a)(1 - \alpha \sin \pi y/a)$. Two cases of $\alpha = 0.3$ and $\alpha = 0.5$ are considered. It shows that the frequency parameters will decrease with the increase of $\alpha$. The

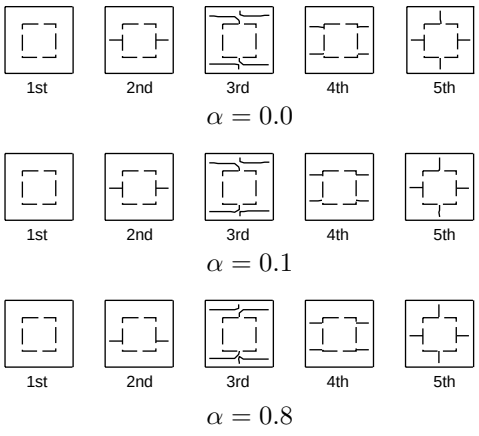


**Fig. 7** Nodal patterns for SSSS orthotropic square plate with a square hole and variable thickness in one direction ($c/a = 0.5, a/h = 100, h_0/h_t = 12$).

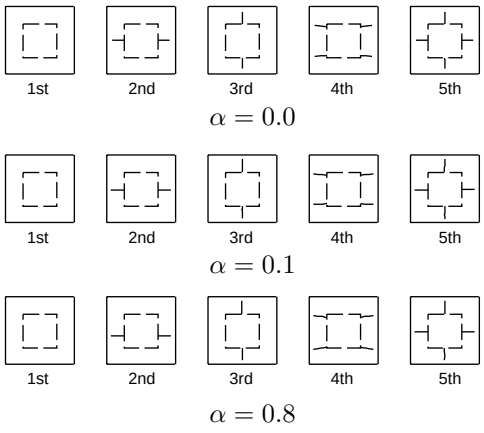


**Fig. 8** Nodal patterns for SSSS orthotropic square plate with a square hole and variable thickness in one direction ($c/a = 0.5, a/h = 10, h_0/h_t = 14$).

nodal patterns of the 5 modes of the plates are shown in Figures 9 and 10.

## 7. Conclusions

An approximate method is extended for analyzing the free vibration problem of simply supported orthotropic square plate with a square hole. An equivalent square plate is used to obtain the dynamic characteristics of a plate with a hole. The characteristic equation of the free vibration is gotten by using the Green function. The frequency parameters and their mode shapes are shown for simply supported thin and moderately thick plates with a hole for isotropic and

**Table 9** Natural frequency parameter $\lambda$ for SSSS orthotropic square plate with a square hole and variable thickness in two directions ($c/a = 0.5, a/h_0 = 100, h_0/h_t = 14$)

| | | Mode sequence number | | | | |
|---|---|---|---|---|---|---|
| $\alpha$ | Source | 1st | 2nd | 3rd | 4th | 5th |
| 0.3 | Present | 6.289 | 7.634 | 8.286 | 9.578 | 12.520 |
| 0.5 | Present | 5.691 | 6.994 | 7.759 | 8.927 | 11.454 |

**Table 10** Natural frequency parameter $\lambda$ for SSSS orthotropic square plate with a square hole and variable thickness in two directions ($c/a = 0.5, a/h_0 = 10, h_0/h_t = 16$)

| | | Mode sequence number | | | | |
|---|---|---|---|---|---|---|
| $\alpha$ | Source | 1st | 2nd | 3rd | 4th | 5th |
| 0.3 | Present | 5.995 | 7.147 | 7.504 | 8.788 | 10.021 |
| 0.5 | Present | 5.543 | 6.705 | 7.124 | 8.395 | 9.755 |

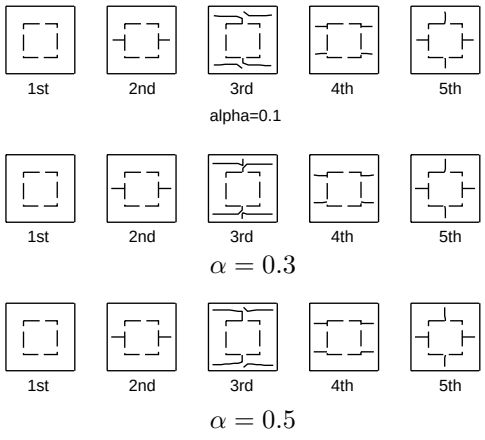


**Fig. 9** Nodal patterns for SSSS orthotropic square plate with a square hole and variable thickness in two directions ($c/a = 0.5, a/h = 100, h_0/h_t = 14$).

orthotropic cases. It can be known that the transverse shear deformation effect is much more pronounced in orthotropic plate than in isotropic plate. The effects of the variation of the thickness in one and two directions on the frequencies are considered. The results by the present method have been compared with those previously reported. It shows that the present results have a good convergence and satisfactory accuracy. Although numerical results are given for only simply supported plates, the present method is a general method and can be used to solve the vibration problem of plates with different boundary conditions.

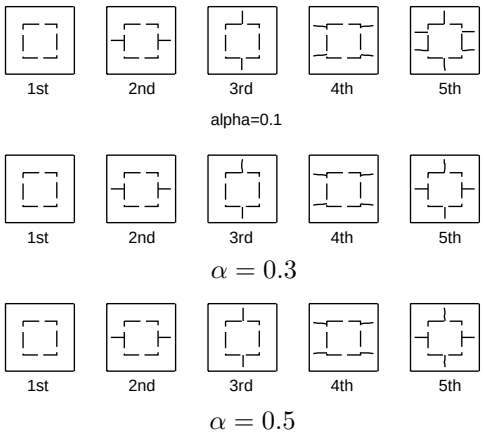


**Fig. 10** Nodal patterns for SSSS orthotropic square plate with a square hole and variable thickness in two directions ($c/a = 0.5, a/h = 10, h_0/h_t = 16$).

## Acknowledgements

The present study was sponsored by the Japan Society for the Promotion of Science (JSPS).

### REFERENCES

1) LEISSA 1969 *Vibration of plates* (NASA SP-160). Washington, D.C.:Office of Technology Utilization, NASA.
2) P. PARAMASIVAM 1973 *Journal of Sound and Vibration* **30**, 173-178. Free vibration of square plates with square openings.
3) R. F. HEGARTY and T. ARIMAN 1975 *Int. J. Solids Structures* **11**, 895-906. Elasto-dynamic analysis of rectangular plates with circular holes.
4) R. ALI and S. J. ATWAL 1980 *Computers and Structures* **12**, 819-823. Prediction of natural frequencies of vibration of rectangular plates with rectangular cutouts.
5) G. AKSU and R. ALI 1976 *Journal of Sound and Vibration* **44**, 147-158. Determination of dynamic characteristics of rectangular plates with cutouts using a finite difference formulation.
6) J. N. REDDY 1982 *Journal of Sound and Vibration* **83**, 1-10. Large amplitude flexural vibration of layered composite plates with cutouts.
7) D. R. AVALOS, H. A. LARRONDO and P. A. A. LAURA 1999 *Journal of Sound and Vibration* **222**, 691-695. Analysis of vibrating rectangular anisotropic plate with free-edge holes.
8) M.HUANG and T.SAKIYAMA 1999 *Journal of Sound and Vibration* **226**, 769-786. Free vibration analysis of rectangular plates with variously-shaped holes.
9) A. KAUSHAL and R. B. BHAT *14th Canadian Congress of Applied Mechanics CANCAM'93*. A comparative study of vibration of plates with cutouts using the finite element and the Rayleigh Ritz methods.
10) K. Y. LAM, K. C. HUNG and S. T. CHOW 1989 *Applied Acoustics* **28**, 49-60. Vibration analysis of plates with cutouts by the modified Rayleigh Ritz method.
11) F. C. APPL and N. R. BYERS 1965 *J.Appl.Mech* **32**, 163-167. Fundamental frequency of simply supported rectangular plates with linearly varying thickness.
12) G. MUNDKUR, R. B. BHAT and S. NERIYA 1994 *Journal of Sound and Vibration* **176**, 136-144. Vibration of plates with cut-outs using boundary characteristic orthogonal polynomial functions in the Rayleigh-Ritz method.
13) G. N. GEANNAKAKES 1995 *Journal of Sound and Vibration* **183**, 441-478. Natural frequencies of arbitrarily shaped plates using the Rayleigh-Ritz method together with natural co-ordinate regions and normalized characteristic orthogonal polynomials.
14) K. M. LIEW, K. C. HUNG and M. K. CLIM 1995 *Journal of Sound and Vibration* **182**, 77-90. Vibration of mindlin plates using boundary characteristic orthogonal polynomials.
15) J. BEUTEL, D. THAMBIRATNAM and N. PERERA 2001 *Engineering Structures* **23**, 1152-1161. Monotonic behaviour of composite column to beam connections.
16) I.M. DANIEL and O. ISHAI 1994 *Engineering Mechanics of Composite Materials*. Oxford university press.

## Appendix A

$F_{111} = F_{123} = F_{134} = 1,$
$F_{146} = \overline{D}_{12}, F_{147} = \overline{D}_{16}$
$F_{156} = \overline{D}_{22}, F_{157} = F_{166} = \overline{D}_{26},$
$F_{167} = \overline{D}_{66}, F_{178} = k\overline{A}_{44}\ F_{188} = k\overline{A}_{45}$
$F_{212} = F_{225} = F_{233} = \mu, F_{246} = F_{267} = \mu\overline{D}_{16},$
$F_{247} = \mu\overline{D}_{11}\ F_{256} = \mu\overline{D}_{26}, F_{257} = \mu, \overline{D}_{12},$
$F_{266} = \mu\overline{D}_{66}\ F_{278} = F_{30907} = F_{31006} = \mu k\overline{A}_{45},$
$F_{288} = F_{387} = \mu k\overline{A}_{55},$
$F_{322} = F_{331} = -\mu,\ F_{345} = F_{354} = F_{363} = -\mu\overline{D}$
$F_{371} = F_{382} = -\mu\overline{DT}$

other$F_{kts} = 0$

## Appendix B

$A_{p1} = \gamma_{p1},\ A_{p2} = 0, A_{p3} = \gamma_{p2},$
$A_{p4} = \gamma_{p3}, A_{p5} = 0,$
$A_{p6} = \overline{D}_{12}\gamma_{p4} + \overline{D}_{22}\gamma_{p5} + \overline{D}_{26}\gamma_{p6},$
$A_{p7} = \overline{D}_{16}\gamma_{p06} + \overline{D}_{26}\gamma_{p07} + \overline{D}_{66}\gamma_{p08},$
$A_{p8} = k(\overline{A}_{44}\gamma_{p7} + \overline{A}_{45}\gamma_{p8})$
$B_{p1} = 0,\ B_{p2} = \mu\gamma_{p1}, B_{p3} = \mu\gamma_{p3},$
$B_{p4} = 0,\ B_{p5} = \mu\gamma_{p2},$
$B_{p6} = \mu(\overline{D}_{16}\gamma_{p4} + \overline{D}_{26}\gamma_{p5} + \overline{D}_{66}\gamma_{p6}),$
$B_{p7} = \mu(\overline{D}_{11}\gamma_{p4} + \overline{D}_{12}\gamma_{p5} + \overline{D}_{16}\gamma_{p6}),$
$B_{p8} = \mu k(\overline{A}_{45}\gamma_{p7} + \overline{A}_{55}\gamma_{p8}),$
$C_{p1kl} = \mu\gamma_{p3} + \mu\overline{DT}_{kl}\gamma_{p7},$
$C_{p2kl} = \mu\gamma_{p2} + \mu\overline{DT}_{kl}\gamma_{p8},$
$C_{p3kl} = \mu\overline{D}_{kl}\gamma_{p6},$
$C_{p4kl} = \mu\overline{D}_{kl}\gamma_{p7},$
$C_{p5kl} = \mu\overline{D}_{kl}\gamma_{p4},$
$C_{p6kl} = -\mu k(\overline{A}_{44}\gamma_{p7} + \overline{A}_{45}\gamma_{p8},$
$C_{p7kl} = -\mu k(\overline{A}_{45}\gamma_{p7} + \overline{A}_{55}\gamma_{p8}),$
$C_{p8kl} = 0\ [\gamma_{pt}] = [\rho_{tp}]^{-1},$
$\rho_{11} = \beta_{ii},\ \rho_{12} = \mu\beta_{jj},\ \rho_{22} = -\mu\beta_{ij},$
$\rho_{23} = \beta_{ii},\ \rho_{25} = \mu\beta_{jj},\ \rho_{31} = -\mu\beta_{ij},$
$\rho_{33} = \mu\beta_{jj},\ \rho_{34} = \beta_{ii},\ \rho_{45} = -\mu\beta_{ij}\overline{D}_{ij},$
$\rho_{46} = \overline{D}_{12}\beta_{ii} + \mu\overline{D}_{16}\beta_{jj},\ \rho_{47} = \overline{D}_{16}\beta_{ii} + \mu\overline{D}_{11}\beta_{jj},$
$\rho_{54} = -\mu\beta_{ij}\overline{D}_{ij},\ \rho_{56} = \overline{D}_{22}\beta_{ii} + \mu\overline{D}_{26}\beta_{jj},$
$\rho_{57} = \overline{D}_{26}\beta_{ii} + \mu\overline{D}_{12}\beta_{jj},\ \rho_{63} = -\mu\beta_{ij}\overline{D}_{ij},$
$\rho_{666} = \overline{D}_{26}\beta_{ii} + \mu\overline{D}_{66}\beta_{jj},\ \rho_{67} = \overline{D}_{66}\beta_{ii} + \mu\overline{D}_{16}\beta_{jj},$
$\rho_{71} = -\mu\beta_{ij}\overline{D}_{ij},\ \rho_{76} = \mu k\overline{A}_{44}\beta_{ij},$
$\rho_{77} = \mu k\overline{A}_{45}\beta_{ij},\ \rho_{78} = k(\overline{A}_{44}\beta_{ii} + \mu\overline{A}_{45}\beta_{jj}),$
$\rho_{82} = -\mu\beta_{ij}\overline{D}_{ij},\ \rho_{86} = \mu k\overline{A}_{45}\beta_{ij},$
$\rho_{87} = \mu k\overline{A}_{55}\beta_{ij},\ \rho_{88} = k(\overline{A}_{45}\beta_{ii} + \mu\overline{A}_{55}\beta_{jj}),$
other $\quad \rho_{tp} = 0$

$$b_{pijfd} = \sum_{t=1}^{13}\Bigg\{\sum_{k=0}^{i}\beta_{ik}A_{pt}[b_{tk0gd} - b_{tkjgd}(1-\delta_{ki})] + \sum_{l=0}^{j}\beta_{jl}B_{pt}[b_{t0lgd} - b_{tilgd}(1-\delta_{lj})] + \sum_{k=0}^{i}\sum_{l=0}^{j}\beta_{ik}\beta_{jl}C_{ptkl}b_{tklgd}(1-\delta_{ki}\delta_{lj})\Bigg\}$$

$$\overline{q}_{pij} = \sum_{t=1}^{13}\Bigg\{\sum_{k=0}^{i}\beta_{ik}A_{pt}[\overline{q}_{tk0} - \overline{q}_{tkj}(1-\delta_{ki})] + \sum_{l=0}^{j}\beta_{jl}B_{pt}[\overline{q}_{t0l} - \overline{q}_{til}(1-\delta_{lj})] + \sum_{k=0}^{i}\sum_{l=0}^{j}\beta_{ik}\beta_{jl}C_{ptkl} - A_{p1}u_{iq}u_{jr}$$

## Appendix C

$a_{1i0i01} = a_{3i0i02} = a_{4i0i03} = 1, \quad a_{6i0i04} = a_{7i0i05} = a_{8i0i06} = 1$

$b_{20jj01} = b_{30jj02} = b_{50jj03} = 1, \quad b_{60jj04} = b_{70jj05} = b_{80jj06} = 1, \quad b_{300002} = 0$

$$a_{pijfd} = \sum_{t=1}^{13}\Bigg\{\sum_{k=0}^{i}\beta_{ik}A_{pt}[a_{tk0fd} - a_{tkjfd}(1-\delta_{ki})] + \sum_{l=0}^{j}\beta_{jl}B_{pt}[a_{t0lfd} - a_{tilfd}(1-\delta_{lj})] + \sum_{k=0}^{i}\sum_{l=0}^{j}\beta_{ik}\beta_{jl}C_{ptkl}a_{tklfd}(1-\delta_{ki}\delta_{lj})\Bigg\}$$